CHRONOLOGY OF HESPERIA PLANUM, MARS: NEW CONSTRAINTS USING IMPACT CRATERS AS STRATIGRAPHIC MARKERS. S. C. Mest[1,2] and D. A. Crown[1], [1]Planetary Science Institute, Tucson, AZ (mest@psi.edu); [2]NASA Goddard Space Flight Center, Greenbelt, MD.

Introduction: Impact craters represent temporally and stratigraphically distinct events in the geologic record of a planetary surface. They can be used to constrain the local and regional geologic history by combining relative and absolute age estimates for crater materials with observations of cross-cutting relationships between impact craters and other geologic features. Model ages derived for impact crater materials in Hesperia Planum (HP) are providing important temporal constraints on emplacement of the ridged plains material, ridge-forming events, and fluvial modification of the plains. This abstract presents results obtained from analyses of several large impact craters in the Hesperia Planum region.

Geologic Setting: Hesperia Planum (> 2 million km^2 in area) is characterized by a high concentration of mare-type wrinkle ridges and ridge rings [1-4]. Most of HP occurs between 1000 and 2000 meters in elevation; Eridania Planitia, located in southeast HP, forms a depression 0 to 1000 m in elevation. Hesperia Planum is stratigraphically significant and has been used to define the base of the Hesperian System [1,5]. Geologic mapping studies at local [6-8] and regional [e.g., 2,9-12] scales have identified areas within HP that do not represent typical "ridged plains." Some areas have been remapped as part of Tyrrhenus Mons, and other areas appear to have been formed or at least modified by fluvial processes. As a result, large areas of ridged plains within HP have been reclassified, suggesting a more complex and diverse geologic history.

Approach: This study is compiling crater size-frequency distribution statistics of materials associated with relatively fresh craters in HP that could serve as important stratigraphic markers. Similar studies in Deuteronilus Mensae [13,14] have provided temporal constraints on the formation of the highland-lowland boundary, fretted terrain development, and emplacement of lobate debris aprons.

In this study, we select craters that are greater than 15 km in diameter, isolated from adjacent young craters, display pristine morphologies, and sufficiently covered by high-resolution images. The availability of high-resolution images allows us to characterize crater populations at diameters as small as 50 m for determination of relative and absolute ages. The THEMIS daytime IR mosaic (100 m/pixel) serves as the regional base. We use high-resolution CTX (~5 m/pixel) and THEMIS VIS (~18 m/pixel) images to map materials associated with specific craters and identify and measure superposed craters; HiRISE (~1-2 m/pixel) and MOC (~2-12 m/pixel) images are used as needed.

Images are imported into ArcGIS for each crater analyzed. The margins of the continuous ejecta blanket, crater rim, and crater floor deposits are mapped, and the diameters of superposed craters are measured. ArcGIS is being used to calculate unit areas and record crater diameters. Crater size-frequency distribution statistics are compiled using the methodology described in [15-18]; all craters (D>50 m) on a given surface are counted while avoiding obvious secondary craters and secondary rays, chains, or clusters. These data are plotted on isochrons [16-18] to assess relative age (Martian time-stratigraphic age) and estimate absolute age. The production function used to determine the isochrons includes both primaries and a component of "background" secondaries (i.e., secondaries not included in rays, chains or clusters) [16-18]. Cumulative crater statistics (i.e., N(2) and N(5), [7]) are also determined for comparison to statistics compiled in previous geologic mapping studies [1,2,6,7].

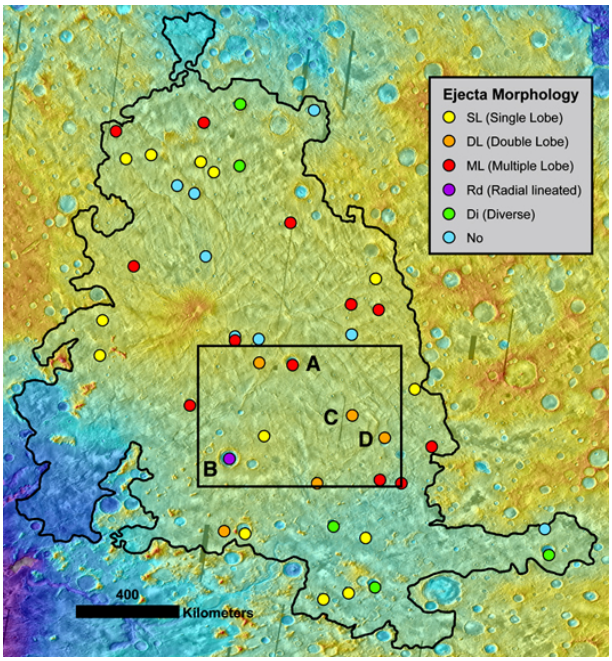

Figure 1. Map of HP (black boundary) and 44 pristine craters; 'Ejecta Morphology' defined by [19,20]. Box indicates location of Figure 2, which shows Kinkora (A), Pál (B), and unnamed craters 1 (C) and 2 (D).

Results: We have identified 44 craters in HP that meet our criteria for analysis (Fig. 1). Craters Kinkora, Pál, and two unnamed craters have been evalued, and their results are presented here. Shown in Figure 2, Kinkora (D=47 km) exhibits multi-lobe ejecta morphology, Pál (D=73 km) exhibits radial lineated

ejecta morphology, and craters 1 and 2 (both ~15 kilometers in diameter) exhibit double-lobe ejecta morphologies.

Crater size-frequency distribution statistics for these four craters are shown in Figure 3; all superposed craters with diameters greater than 50 m were measured for Kinkora (N=14,691), 1 (N=735) and 2 (N=728), but due to the degree of eolian modifation of Pál's ejecta, only craters greater than 1 km in diameter were measured for Pál (N=103). Statistics for Kinkora, crater 1, and Pál show a strong fit to the Noachian-Hesperian boundary, especially for diameters greater than ~200 meters, which is consistent with regional and local mapping studies. For example, recent mapping of southern parts of Hesperia Planum [6] has shown that the plains are Early Hesperian to Late Noachian in age and that a significant amount of fluvial modification post-dates plains emplacement. However, crater 2, although similar in area and number of superposed craters, appears younger (Late Amazonian) due to a large number of smaller diameter craters. The rollover for Kinkora, 1 and 2 is likely due to burial of smaller diameter craters by eolian materials.

Summary: High-resolution images are providing important constraints on the relative ages of fresh impact craters. The results of this study are being used to constrain the ages of the underlying plains materials within HP and evaluate the timing of wrinkle ridge formation within the plains. Dating multiple craters throughout HP will enable us to evaluate hypotheses for the origin(s) of reclassified HP materials.

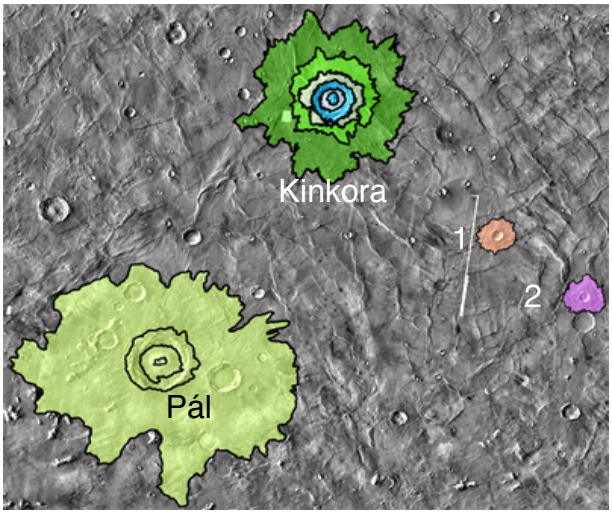

Figure 2. THEMIS daytime IR mosaic of Hesperia Planum showing craters Kinkora, Pál, 1 and 2.

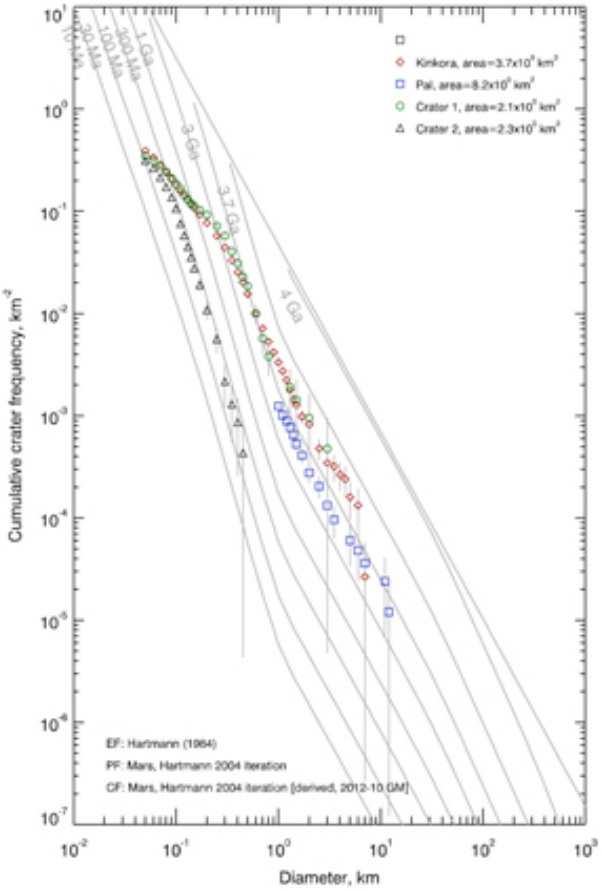

Figure 3. Crater size-frequency distribution plots for craters Kinkor, Pál, and craters 1 and 2.

References: [1] Greeley, R., and J.E. Guest (1987) USGS Misc. Inv. Ser. Map, I-1802-B. [2] Tanaka, K.L., and G.J. Leonard (1995) *JGR*, **100**, 5407-5432. [3] Potter, D.B. (1976) USGS Geol. Invest. Ser. Map I-941, 1:5M scale. [4] King, E.A. (1978) USGS Geol. Invest. Ser. Map I-1073. [5] Tanaka, K.L. (1986) *JGR Suppl.*, **91**, E139-E158. [6] Mest, S.C., and D.A. Crown (2002) USGS Geol. Inv. Ser. Map I-2730. [7] Mest, S.C., and D.A. Crown (2003) USGS Geol. Inv. Ser. Map I-2763. [8] Mest, S.C. and D.A. Crown (2012) *Geologic Map of MTM -30247, -35247 and -40247 Quadrangles, Reull Vallis Region of Mars*, USGS Geol. Surv. Sci. Inv. Map 3245. [9] Crown, D.A., et al. (1992) *Icarus*, **100**, 1–25. [10] Mest, S.C., and D.A. Crown (2001) *Icarus*, **153**, 89-110. [11] Gregg, T.K.P., and D.A. Crown (2009) NASA/CP—2010–216680, 27-28. [12] Ivanov, M.A., et al. (2005) *JGR*, **110**, E12S21, doi:10.1029/2005JE002420. [13] Berman, D.C., et al. (2011) 42nd LPSC, **#1435**. [14] Joseph, E.C.S., et al. (2011) 42nd LPSC, **#1206**. [15] Berman, D.C. and W.K. Hartmann (2002) *Icarus*, **159**, doi:10.1006/icar.2002.6920. [16] Hartmann, W.K. (2005) *Icarus*, **174**, 294-320. [17] Hartmann, W.K. (2007) 7th Intl. Conf. on Mars, **#3318**. [18] Hartmann, W.K. (2007) *Icarus*, **189**, 274-278. [19] Barlow, N.G. (2003 6th Intl. Conf. on Mars, **3073**. [20] Barlow, N.G. (2006) 37th LPSC, **#1337**.